Oxygen stoichiometry and magnetic properties of LuFe2O4+δ

Fan Wang, Jungho Kim, G. D. Gu, Yongjae Lee, Saebyok Bae et al.

Related Articles

Magnetization model for a Heusler alloy
J. Appl. Phys. 113, 17A915 (2013)

Enhancement of ferromagnetism by Cr doping in Ni-Mn-Cr-Sb Heusler alloys
Appl. Phys. Lett. 102, 112402 (2013)

Magnetic properties of nanostructured Fe-Co alloys
J. Appl. Phys. 113, 113905 (2013)

Injection locking at zero field in two free layer spin-valves
Appl. Phys. Lett. 102, 102413 (2013)

Ac susceptibility studies of a superconducting gallium nanocomposite: Crossover in the upper critical field line and activation barriers
J. Appl. Phys. 113, 113903 (2013)

Additional information on J. Appl. Phys.

Journal Homepage: http://jap.aip.org/

Journal Information: http://jap.aip.org/about/about_the_journal

Top downloads: http://jap.aip.org/features/most_downloaded

Information for Authors: http://jap.aip.org/authors

Oxygen stoichiometry and magnetic properties of LuFe$_2$O$_{4+\delta}$

Fan Wang,[1] Jungho Kim,[1,a)] G. D. Gu,[2] Yongjae Lee,[3] Saebyok Bae,[1,4] and Young-June Kim[1,b)]

[1]*Department of Physics, University of Toronto, Toronto, Ontario M5S1A7, Canada*
[2]*Department of Condensed Matter and Material Science, Brookhaven National Laboratory, Upton, New York 11973, USA*
[3]*Department of Earth System Sciences, Yonsei University, Seoul 120-749, Korea*
[4]*Global Institute for Talented Education, KAIST, KAIST ICC Munji Campus, 103-6 Munji-dong, Yuseong-gu, Daejeon 305-732, Korea*

We report a comprehensive investigation of the magnetic properties of LuFe$_2$O$_4$ (LFO) samples with different oxygen stoichiometries. Samples with excess oxygen exhibit spin glass behavior without long-range magnetic order, while three-dimensional ferrimagnetic order exists in a stoichiometric sample. Dissimilar experimental observations reported in several papers can be understood consistently when oxygen stoichiometry is taken into account. The stoichiometric sample orders magnetically below T$_N$ = 243 K, and a monoclinic lattice distortion sets in below T$_L$ = 175 K. This structural change is sensitive to the applied magnetic field, indicating strong spin-lattice coupling in this material. Unusual low-field thermal magnetization behavior was observed near T$_L$, and its origin is discussed. © *2013 American Institute of Physics*. [http://dx.doi.org/10.1063/1.4792036]

I. INTRODUCTION

The physics of LuFe$_2$O$_4$ (LFO) has drawn much attention recently due to its fascinating magnetic and electronic properties.[1–19] Electron, x-ray, and neutron diffraction experiments show that there is both charge order (CO) and spin order (SO) in LFO.[3,6,10] It has been suggested that LFO could be a multiferroic compound based on the observation of charge order driven ferroelectricity,[7] a large magneto-dielectric response,[8] and an anomalously large pyroelectric signal near the SO temperature.[7] However, the details of the charge and spin ordering are complex and understanding its magnetic properties has been quite challenging. In isostructural YFe$_2$O$_4$, two first order structural transitions at ~230 K and 190 K were found, corresponding to transitions from hexagonal to monoclinic, and monoclinic to triclinic, respectively.[20] However, a recent x-ray powder diffraction study has revealed that there are in fact more than two structural transitions in YFe$_2$O$_4$.[21] In addition, neutron scattering experiments reported that oxygen non-stoichiometry plays an important role in determining the magnetic properties of YFe$_2$O$_4$.[22,23] Stoichiometric YFe$_2$O$_4$ shows a three-dimensional (3D) spin order, while non-stoichiometric YFe$_2$O$_4$ exhibits only two-dimensional (2D) magnetic correlation.[22–24]

Recent magnetization and neutron scattering experiments show that different LFO samples also exhibit significantly different magnetic properties, presumably due to the difference in the oxygen content.[3,25,26] According to Ref. 1, there is no 3D magnetic ordering in this system even down to 4.2 K, and only 2D ferrimagnetic clusters are formed below 220 K. On the other hand, in a recent neutron experiment, Christianson *et al.* found 3D magnetic Bragg peaks at (1/3,1/3,L) with integer L below 240 K (T$_H$).[3] To explain the

observation, they proposed a magnetic structure, in which a ferrimagnetic order in the ab plane is stacked ferromagnetically (FM) along the c axis. Another first order transition was observed at ~175 K (T$_L$), below which the magnetic peak intensity drops abruptly and the c-axis magnetic correlation length decreases. This transition was also observed in their thermal magnetization data as a broad feature above T$_L$. Based on this observation, Christianson *et al.* argued that a structural change occurs at T$_L$, and the stacking disorder induced by this structural change leads to local antiferromagnetic (AFM) stacking of ferrimagnetic layers below T$_L$. As a result, magnetic peak intensity, correlation length, and magnetization all decrease in this temperature range. X-ray scattering experiments by Xu *et al.* confirmed that a monoclinic lattice distortion happens below T$_L$.[4] They also showed that the lattice distortion could be suppressed by applying magnetic field. The amplitude of the critical field H$_c$, beyond which the lattice distortion is suppressed, depends on whether the field is swept up or down. The critical field values obtained from the magnetization measurements were found to increase with decreasing temperature, in agreement with that determined from their x-ray experiment. These recent neutron and x-ray results contradict earlier studies by Iida and coworkers.[1] In addition, a recent high field magnetization study by Wu *et al.*[2] and Patankar *et al.*[27] found results similar to the earlier data by Iida *et al.* These different experimental results seem to suggest that physical properties of LFO are strongly sample dependent, similar to the case of YFe$_2$O$_4$.[22,23]

In their recent structural studies, Bourgeois *et al.* found that a structural modulation due to excess oxygen could be present in such a nonstoichiometric sample; this modulation seems to disappear when annealed under vacuum.[25] Strong sample dependent magnetic properties have been also noted by de Groot and coworkers,[26] while Patankar and coworkers noted that magnetic properties do not change much under

a)Current address: XOR, Advanced Photon Source, Argonne Nation Laboratory, Argonne, Illinois 60439, USA.
b)Electronic mail: yjkim@physics.utoronto.ca.

annealing in air at 350 °C for 1 h.[27] In our comprehensive investigation of magnetic properties of LFO using DC magnetization, AC susceptibility, and specific heat, it was clear that different samples of nominally stoichiometric LFO exhibited significantly different behavior and could be broadly classified into two types of samples depending on their magnetic ground states. From our thermogravimetric analysis (TGA), we found that there was a small difference in oxygen stoichiometry between these two sample types. Samples with excess oxygen were characterized as a spin glass phase, and its thermal magnetization was similar to the result of Iida *et al.*[1] More stoichiometric samples exhibited magnetically ordered ground states, and their thermal magnetization data were consistent with the result of Christianson *et al.*[3] The spin glass (SG) behavior was investigated thoroughly in our previous study and reported in Ref. 5.

In this paper, we present a comprehensive characterization of the second type of samples: those with stoichiometric oxygen concentrations. In contrast to the sample with excess oxygen, neither DC magnetization nor AC susceptibility shows spin glass behavior. In addition, the magnetization vs. applied field data show an unusual two-step feature, in contrast to the earlier results reported by Wu *et al.* and Iida *et al.*[2,3] A monoclinic structural distortion is also observed at ∼175 K in both powder and single crystal x-ray diffraction experiments on this stoichiometric sample, while the sample with excess oxygen shows no structural change. We could therefore explain widely different physical properties observed in the literature[1–4] by differences in sample quality, most likely due to the difference in the oxygen concentration.

II. EXPERIMENTAL METHODS

LFO single crystals were grown using the travelling solvent floating zone method as described in Ref. 28. During our investigation, we realized that there were two types of samples exhibiting distinct magnetic properties. Note that all crystals studied here came from the same batch without any annealing procedure, and some crystals show mixed magnetic behavior of these two types. In order to characterize possible oxygen non-stoichiometry, we carried out thermogravimetric analysis (TGA) in reducing atmosphere (5% H_2:Ar) up to about 1025 °C, at which temperature the LFO sample decomposes into Lu_2O_3 and Fe. We found that the oxygen concentration of the sample showing spin glass behavior is ∼4.07 ± 0.03 (labeled as $\delta = 0.07$ sample).[5] The other sample's stoichiometry was found to be much closer to 4.0, although accurate determination was not possible. We will label this sample as $\delta = 0$. It is easy to distinguish between the two types of samples, thanks to distinct low-field magnetic properties. Most of the measurements in this report were done on two pieces of $\delta = 0$ samples, using quantum design magnetic property measurement system (MPMS). High magnetic field measurements were carried out using the quantum design physical property measurement system (PPMS) with a 14 T superconducting magnet. In order to characterize the structural phase transition in the $\delta = 0$ sample, temperature-dependent x-ray powder diffraction measurements were carried out at the HRPD beamline at Pohang

Accelerator Laboratory (PAL) using 8.0 keV photons. X-ray diffraction experiments on single crystal samples were carried out at the X21 beamline at the National Synchrotron Light Source in Brookhaven National Laboratory using 15 keV photons.

III. EXPERIMENTAL RESULTS

A. Zero field properties

X-ray powder diffraction patterns for the $\delta = 0$ sample obtained at different temperatures are shown in Fig. 1. At temperatures below 200 K, the (1,0,1) and (1,0,4) peaks split, indicating that there is a structural change between 150 K and 200 K. The structure of this system was analyzed using the general structure and analysis system (GSAS) software. At high temperatures, LFO belongs to a rhombohedral space group $R\bar{3}m$ as reported in Ref. 29. However at low temperatures, the data could not be fitted satisfactorily with the $R\bar{3}m$ nor any other space group. The best fit was obtained when we assumed that about half of the sample was in $C2/m$ (monoclinic) space group, while the rest remained in $R\bar{3}m$, suggesting that a partial structural distortion may be occurring. The structure was refined with the $C2/m$ space group in a recent x-ray structural study.[25] We note that the $\delta = 0.07$ sample does not show such a structural transition. To check if the observed peak splitting is due to the texture of the powder sample, we studied a single crystal sample. Fig. 2 shows θ-2θ scan around the (2,0,2) peak from our single crystal x-ray diffraction. It clearly shows that at 165 K a two peak feature shows up, confirming that the structure change is intrinsic for this type of sample. Similar structural distortion was observed with x-ray diffraction in Ref. 4; Xu *et al.* also observed that the transition temperature, T_L, below which the distortion appears, depends on the strength of the applied magnetic field.

B. Low field properties

The LFO sample showed quite unusual magnetic behavior when a small field was applied. Figure 3(a) shows zero-field cooled (ZFC) and field cooled (FC) DC magnetization of the
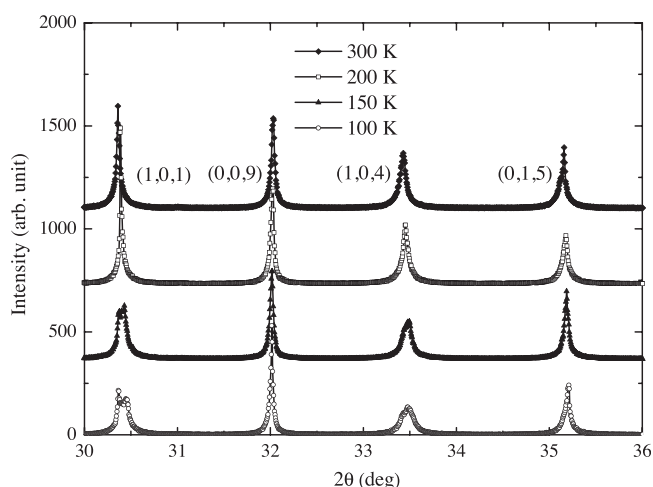

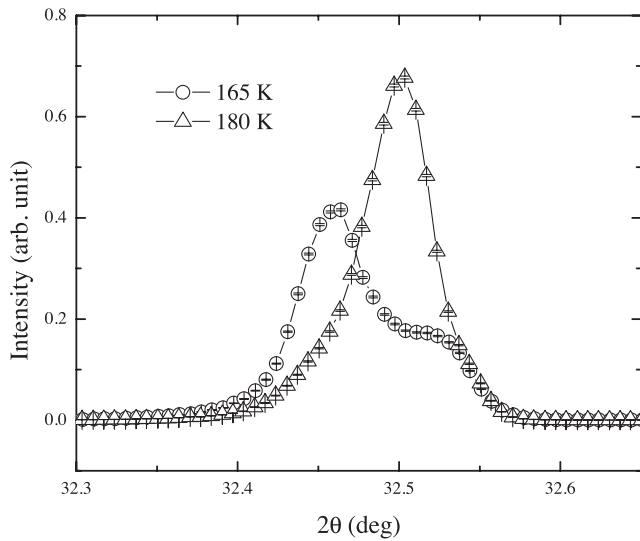FIG. 1. X-ray powder diffraction patterns at different temperatures.

FIG. 2. θ-2θ scan around (2,0,2) peak at 180 K and 165 K obtained from single crystal x-ray diffraction.

$\delta = 0.07$ and $\delta = 0$ samples measured in the temperature range from 2 K to 300 K when a 10 Oe magnetic field was applied. The magnetization of the $\delta = 0.07$ sample shows a peak at ~237 K, and below this temperature, the FC magnetization begins to deviate from the ZFC magnetization. As reported in Ref. 5, the transition around 237 K is due to a paramagnetic to ferrimagnetic transition; at lower temperature, the $\delta = 0.07$ sample exhibits highly relaxational magnetic behavior due to the spin-glass phase. In contrast, the $\delta = 0$ sample exhibits a number of different properties. First, the ferrimagnetic transition temperature is higher: a sharp peak appears at higher temperature ~243 K with smaller magnitude. Since the $\delta = 0.07$ sample shows a transition around 237 K, excess oxygen seems to suppress the ferrimagnetic transition temperature. The second difference is that between 175 K and 235 K, the ZFC magnetization data are larger than the FC data. The latter is more or less featureless, while a step-like change in the ZFC magnetization is observed around 220 K.
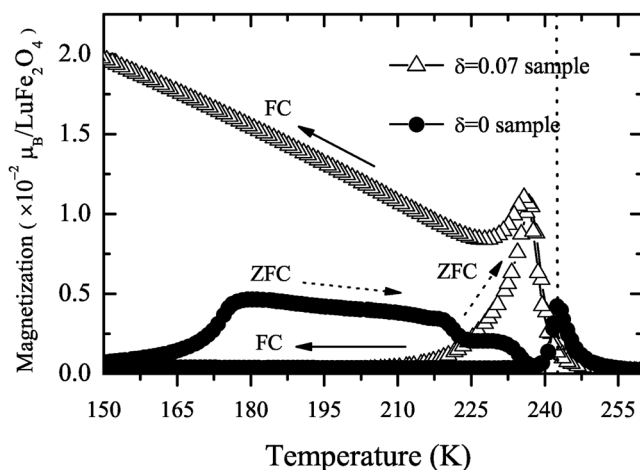
This ZFC DC magnetization behavior was first observed in Ref. 30, and it was called a "field-heating" (FH) effect, since the ZFC data shown in Fig. 3 were obtained by measuring magnetization with a 10 Oe applied field while "heating" the sample after a cool-down in zero external field. To check this, we show our AC susceptibility data as a solid line in Fig. 4, which was obtained while heating the sample under zero external field after initial zero-field cooling. This can be considered as a true ZFC result. This clearly demonstrates that the observed large bump at 175 K is due to field-heating. We carried out a systematic study of this field-heating effect dependence on the initial cool-down temperature (T_s). The sample was initially cooled in zero field to T_s, then a 10 Oe external field was applied and DC magnetization was measured while heating the sample. This ZFC-FH result is plotted in Fig. 4. When T_s is above 175 K, the ZFC-FH curve is similar to the FC curve (Fig. 3(a)), but when $T_s < 175$ K, the ZFC-FH magnetization gradually increases with increasing temperature until the sample reaches 175 K, at which point the magnetization suddenly jumps to a large value and reaches maximum $M_{max}(T_s)$ at ~180 K. The dependence of $M_{max}(T_s)$ on T_s is shown in the inset of Fig. 4. As T_s decreases, $M_{max}(T_s)$ increases. This effect is quite remarkable, since this implies that the sample remembers the lowest temperature in the cooling history, T_s. As discussed in Sec. III A, the structural distortion temperature in this sample is ~175 K, suggesting that the "field-heating" effect may be related to the structural change. We will discuss this further in Sec. IV.

To compare magnetic behavior between the $\delta = 0.07$ and $\delta = 0$ samples, we show AC susceptibility data for both samples in Fig. 5. One of the clear signs of the spin glass behavior in the $\delta = 0.07$ sample is the large imaginary part of the AC susceptibility (χ''). However, χ'' of the $\delta = 0$ sample is almost negligible. In addition, a large frequency

FIG. 3. Thermal magnetization curves measured with a 10 Oe magnetic field, applied parallel to the c-axis.
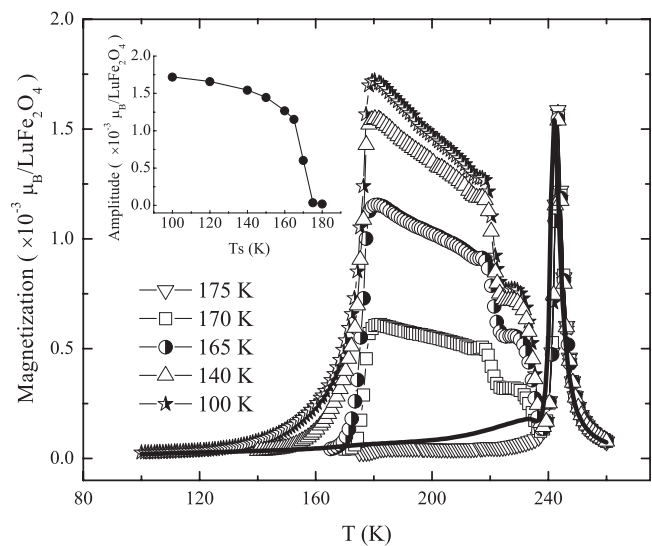

FIG. 4. ZFC magnetization curves of different T_s under a 10 Oe magnetic field parallel to the c axis. The sample was cooled from 260 K to T_s, and then the measurement was taken during heating. The thick solid line is the AC susceptibility measured with zero external field after ZFC. The inset shows the T_s dependence of $M_{max}(T_s)$ obtained from different curves at 180 K. The solid line of the inset is a guide to the eye.
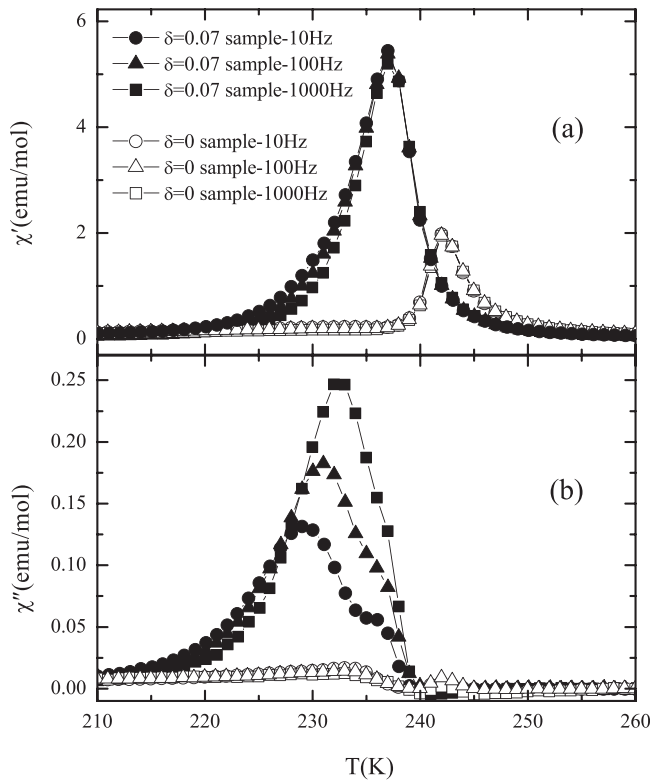
FIG. 5. Temperature dependence of the AC magnetic susceptibility of $\delta = 0.07$ and $\delta = 0$ samples obtained under AC fields of different frequencies with amplitude $h_{ac} = 1$ Oe. Panel (a) and (b) show the real (χ') and imaginary (χ'') parts of the AC susceptibility, respectively.

FIG. 6. DC magnetization measured with higher magnetic fields applied parallel to the c-axis. (a) ZFC-FH magnetization (b) FC magnetization.

dependence of χ' and χ'' is apparent in the temperature range of 220 K–233 K for the $\delta = 0.07$ sample, while the $\delta = 0$ sample does not show any significant frequency dependence, suggesting that $\delta = 0$ sample does not become a spin-glass at this temperature range. One can see that some small χ'' contribution exists in the $\delta = 0$ data. Sometimes even bigger χ'' contributions have been observed for other sample pieces. However, we observed mostly two extreme types of behavior, and the intermediate behavior was rarely observed. This suggests that the samples contain a mixture of $\delta = 0$ and $\delta = 0.07$ phases, rather than a continuous distribution of oxygen concentration. This observation also implies that there could be a miscibility gap between the two phases, and further systematic investigation of the phase diagram would be desirable. We would like to mention that the sample dependent magnetic behavior was also pointed out by de Groot *et al.*[26]

C. High field phase diagram

Thermal magnetization data measured with higher fields are shown in Fig. 6. For the ZFC-FH magnetization shown in panel (a), at low fields, there are two features: a sharp peak at ~243 K and a bump between 175 K and 236 K. As the field increases, the peak broadens and shifts to lower temperature; the two features gradually merge and only a single broad feature remains for the fields above 3000 Oe. For the FC magnetization in panel (b), the low-field magnetization is similar to the one in Fig. 3(a) with only a sharp peak at ~243 K. Above 1000 Oe, the magnetization curve
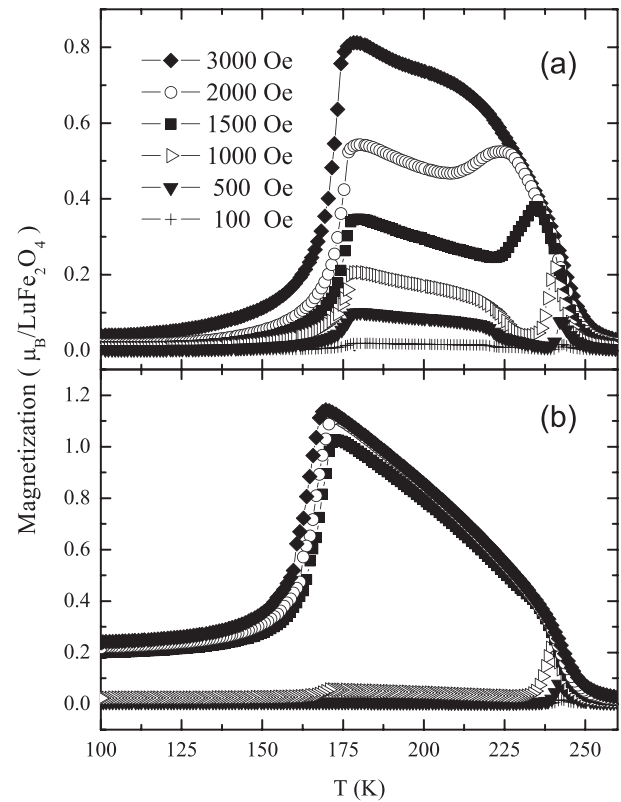
abruptly changes to resemble that of the ZFC-FH data. At H ~ 3000 Oe, the difference between the ZFC-FH and the FC data almost disappears.

In Fig. 7, we show the temperature dependence of the thermomagnetization of the $\delta = 0$ sample obtained with an 1 T field applied parallel or perpendicular to the c axis. The in-plane magnetization is almost 30 times smaller than the c axis magnetization. The possible sample misalignment with respect to the field direction (less than 2°) can entirely account for this small magnetization along the ab-plane.
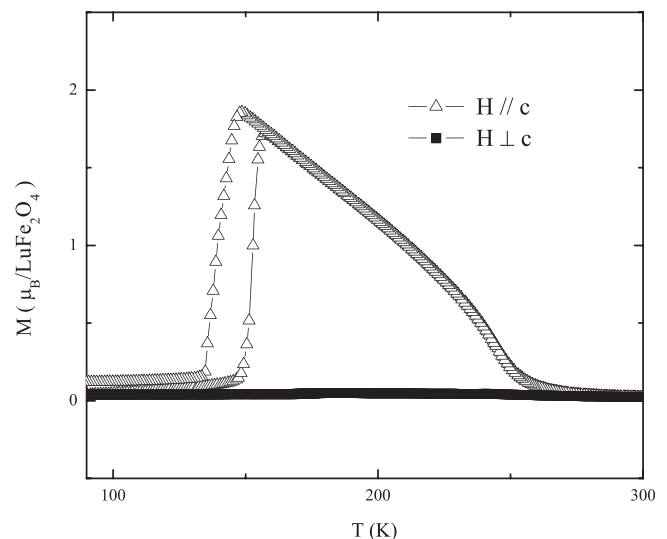

FIG. 7. Temperature dependence of magnetization measured with 1 T field applied parallel or perpendicular to the c axis, respectively.

Therefore, we conclude that strong uniaxial anisotropy along the c axis, which was observed in the $\delta = 0.07$ sample,[5] is also present in the $\delta = 0$ sample.

To investigate field dependence, isothermal magnetization curves obtained at different temperatures are shown in Fig. 8. At 243 K, the magnetization curve is reversible. As temperature decreases, hysteresis behavior shows up, and both the coercive field and the saturation magnetization increase. We note that the coercive field of the $\delta = 0$ sample is much smaller than that of the $\delta = 0.07$ sample.[1] As expected, the low field behavior (inset) depends on the cooling-heating history of the sample. When the sample is directly cooled to 180 K (circle), the magnetization is smaller than the data obtained by cooling the sample to 100 K first and then heated up to 180 K without field. This result is consistent with the ZFC-FH effect shown in Fig. 4. The shapes of the M vs H curves for T = 180 K and T = 100 K are very peculiar. For T = 180 K, there is clearly a coercive field of about 3000 Oe. At a lower temperature, T = 100 K, the coercive field becomes larger, and additionally, a double hysteretic behavior appears, which is reminiscent of the behavior observed for the bidomain state in exchange biased FeF$_2$/Ni.[31] We note that very different M vs. H curves were observed in Refs. 1, 2, and 27, suggesting that these two types of samples exhibit distinct high-field properties.

In order to investigate the high-field behavior further, we measured the ZFC magnetization under high magnetic fields (up to 14 T), which is shown in Fig. 9. The overall shape of the temperature dependence is similar to the data shown in Fig. 6(a). However, the temperature at which the unusual broad feature is turned on, T_L, shifts with changing magnetic field. We define this "transition" temperature from the inflection point of Fig. 9, and its field dependence is plotted in Fig. 10. With increasing magnetic field, T_L is suppressed rapidly. The phase boundary is very well described by a phenomenological exponential curve as shown in Fig. 10.

FIG. 9. ZFC-FH magnetization under high magnetic fields applied along the c axis in a temperature range from 10 K to 260 K.

IV. DISCUSSION

Our central finding is that there are two types of LFO samples with significantly different magnetic properties, and one can distinguish them easily from their thermal magnetization data obtained under small magnetic field. The excess oxygen ($\delta = 0.07$) sample shows a spin glass transition below 237 K.[5] Magnetic properties of the $\delta = 0.07$ sample are similar to the results of Iida *et al.* and Wu *et al.*[1,2] There is no 3D long range magnetic ordering in this type of samples, and at low temperatures, a giant magnetic coercivity was observed.[1,2,16] On the other hand, the stoichiometric sample ($\delta = 0$) exhibits a 3D magnetic ordering. Low-field thermal magnetization in this type of sample shows an unusual behavior; that is, between 175 K and 235 K, and the ZFC magnetization measured while heating in external field exhibits a two-step feature and is much larger than the FC magnetization. This behavior is similar to
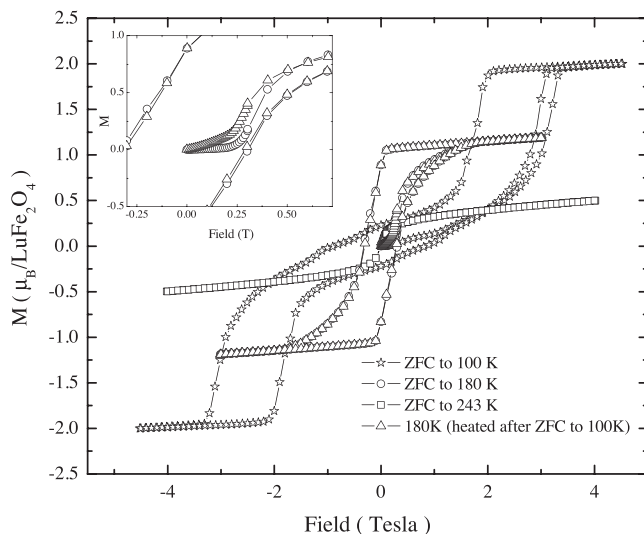

FIG. 8. Isothermal magnetization curves along the c axis at various temperatures after ZFC. The triangular symbol curve was measured at 180 K after cooling the sample to 100 K first and then heating up to 180 K without magnetic field.
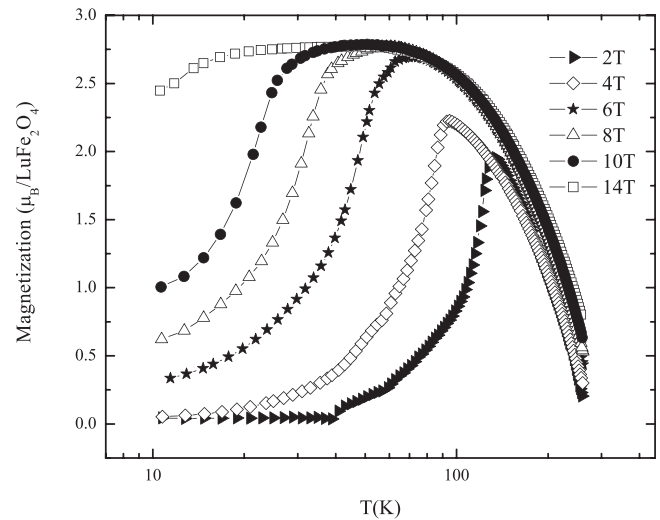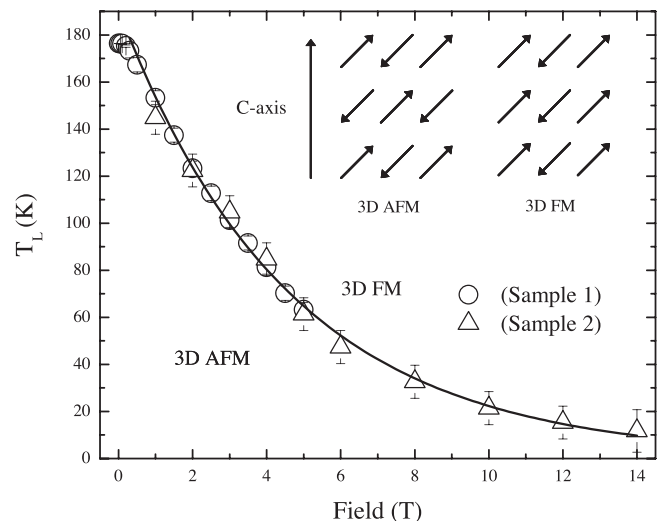

FIG. 10. Field dependence of T_L as a function of applied field along the c direction. The measurement was repeated for two samples. The solid line is an exponential function as a guide: $\sim e^{-H/H_0}$, $H_0 = 4.6$ T. The transition at T_L is from 3D antiferromagnetic to 3D ferromagnetic arrangements of spins along the c axis shown in the inset.

the one observed in Refs. 3 and 4. According to the neutron experiment by Christianson *et al.*, there is a local AFM ordering induced by the lattice distortion below 175 K,[3] which was subsequently identified as a monoclinic lattice distortion in the x-ray scattering experiments by Xu *et al.*[4] They further showed that the structural distortion can be suppressed by magnetic field, and the critical field H_c required for the suppression shows magnetic hysteresis.[4] The H_c obtained from the x-ray experiment is consistent with the one observed in our high-field magnetization measurement (Fig. 10).

Our results, taken together with the neutron and x-ray measurements reported in Refs. 3 and 4, provide the following physical picture for the $\delta = 0$ sample: At zero applied field, a ferrimagnetic in-plane order sets in around 243 K. Such ordered layers are stacked FM along the c axis above 175 K (Fig. 10 inset), but AFM stacking becomes favorable below 175 K. At this temperature, T_L, a monoclinic lattice distortion is also observed to occur. However, this structural distortion does not occur uniformly, and only part of the sample goes through such a change in the stacking pattern. From our x-ray powder diffraction, the volume fraction of the monoclinic-distorted region is roughly half of the total sample volume. Likewise, the fraction of the AFM stacked region, which is responsible for the sudden drop in the magnetization (Fig. 4) as well as the drop in the magnetic Bragg peak intensity (Ref. 3), seems to vary among the samples studied. From this, it is tempting to associate the AFM stacking with the structural distortion. But further studies involving proximal local probes would be useful to make this connection more explicit.

Although a microscopic understanding of the relationship between the structural distortion and the AFM stacking is beyond the scope of this paper, strong magnetostriction could be one of the possible origins for the observed behavior. Indirect evidence for such magneto-structural coupling is provided by the fact that the structural distortion is very sensitive to the applied magnetic field, as shown in the x-ray diffraction study.[4] Since the FM domain growth is accompanied by its volume change, when the FM domain size becomes too large, the elastic energy cost due to the volume change could cause domains to break into smaller ones in order to keep the crystal from breaking. Such behavior would not be observed in samples with spin-glass order, since the domain size does not grow large enough for this to happen. Indeed the magnetic domain size becomes smaller below T_L according to a recent neutron study.[3] When external magnetic field is applied, the Zeeman energy can shift the temperature at which the domain configuration changes. In other words, the observed behavior could be a reflection of strong spin-lattice coupling in this material.[4,18]

V. CONCLUSIONS

We have investigated the magnetic properties of $LuFe_2O_4$ systematically using DC magnetization and AC susceptibility. We found that there are two types of $LuFe_2O_{4+\delta}$ samples, exhibiting very different magnetic ground states. Our thermogravimetric analysis shows that these two types have different oxygen concentrations; the excess oxygen sample is labeled $\delta = 0.07$ and the more stoichiometric one is $\delta = 0$. Contrasting physical properties reported in the literature can be resolved if we take into account these two distinct categories of samples. In the $\delta = 0.07$ sample, there is no 3D magnetic ordering, and at low temperature, a spin-glass transition occurs.[1,5] The $\delta = 0$ sample shows 3D magnetic ordering, and there is a monoclinic lattice distortion which shows magnetic hysteresis. The observed unusual thermal magnetization and magnetic hysteresis in this study all seem to be related to the monoclinic structural distortion observed around 175 K.

[1]J. Iida, M. Tanaka, Y. Nakagawa, S. Funahashi, N. Kimizuka, and S. Takekawa, J. Phys. Soc. Jpn. **62**, 1723 (1993).
[2]W. Wu, V. Kiryukhin, H.-J. Noh, K.-T. Ko, J.-H. Park, I. W. Ratcliff, P. A. Sharma, N. Harrison, Y. J. Choi, Y. Horibe, S. Lee, S. P. H. T. Yi, C. L. Zhang, and S.-W. Cheong, Phys. Rev. Lett. **101**, 137203 (2008).
[3]A. D. Christianson, M. D. Lumsden, M. Angst, Z. Yamani, W. Tian, R. Jin, E. A. Payzant, S. E. Nagler, B. C. Sales, and D. Mandrus, Phys. Rev. Lett. **100**, 107601 (2008).
[4]X. S. Xu, M. Angst, T. V. Brinzari, R. P. Hermann, J. L. Musfeldt, A. D. Christianson, D. Mandrus, B. C. Sales, S. McGill, J.-W. Kim, and Z. Islam, Phys. Rev. Lett. **101**, 227602 (2008).
[5]F. Wang, J. Kim, Y. J. Kim, and G. D. Gu, Phys. Rev. B **80**, 24419 (2009).
[6]Y. Yamada, N. Shinichiro, and N. Ikeda, J. Phys. Soc. Jpn. **66**, 3733 (1997).
[7]N. Ikeda, H. Ohsumi, K. Ohwada, K. Ishii, T. Inami, K. Kakurai, Y. Murakami, K. Yoshii, S. Mori, Y. Horibe, and H. Kito, Nature **436**, 1136 (2005).
[8]M. A. Subramanian, T. He, J. Chen, N. S. Rogado, T. G. Calverese, and A. W. Sleight, Adv. Mater **18**, 1737 (2006).
[9]H. J. Xiang and M.-H. Whangbo, Phys. Rev. Lett. **98**, 246403 (2007).
[10]Y. Zhang, H. X. Yang, C. Ma, H. F. Tian, and J. Q. Li, Phys. Rev. Lett. **98**, 247602 (2007).
[11]A. Nagano, M. Naka, J. Nasu, and S. Ishihara, Phys. Rev. Lett. **99**, 217202 (2007).
[12]M. Angst, R. P. Hermann, A. D. Christianson, M. D. Lumsden, C. Lee, M.-H. Whangbo, J.-W. Kim, P. J. Ryan, S. E. Nagler, W. Tian, R. Jin, B. C. Sales, and D. Mandrus, Phys. Rev. Lett. **101**, 227601 (2008).
[13]C. Li, X. Zhang, Z. Cheng, and Y. Sun, Appl. Phys. Lett. **92**, 182903 (2008).
[14]C. Li, X. Zhang, Z. Cheng, and Y. Sun, Appl. Phys. Lett. **93**, 152103 (2008).
[15]A. M. Mulders, S. M. Lawrence, U. Staub, M. Garcia-Fernandez, V. Scagnoli, C. Mazzoli, E. Pomjakushina, K. Conder, and Y. Wang, Phys. Rev. Lett. **103**, 077602 (2009).
[16]K.-T. Ko, H.-J. Noh, J.-Y. Kim, B.-G. Park, J.-H. Park, A. Tanaka, S. B. Kim, C. L. Zhang, and S.-W. Cheong, Phys. Rev. Lett. **103**, 207202 (2009).
[17]C. Li, F. Wang, Y. Liu, X. Zhang, Z. Cheng, and Y. Sun, Phys. Rev. B **79**, 172412 (2009).

[18]J. Wen, G. Xu, G. Gu, and S. M. Shapiro, Phys. Rev. B **80**, 020403 (2009).

[19]J. Wen, G. Xu, G. Gu, and S. M. Shapiro, Phys. Rev. B **81**, 144121 (2010).

[20]Y. Nakagawa, M. Inazumi, N. Kimizuka, and K. Siratori, J. Phys. Soc. Jpn. **47**, 1369 (1979).

[21]N. Ikeda, R. Mori, K. Kohn, M. Mizumaki, and T. Akao, Ferroelectrics **272**, 309 (2002).

[22]J. Akimitsu, Y. Inada, K. Siratori, I. Shindo, and N. Kimizuka, Solid State Commun. **32**, 1065 (1979).

[23]S. Funahashi, J. Akimitsu, K. Siratori, N. Kimizuka, M. Tanaka, and H. Fujishita, J. Phys. Soc. Jpn. **53**, 2688 (1984).

[24]Y. Nakagawa, M. Kishi, H. Hiroyoshi, N. Kimizuka, and K. Siratori, in *Ferrites* (CAPJ, Tokyo, 1981), p. 115.

[25]J. Bourgeois, M. Hervieu, M. Poienar, A. M. Abakumov, E. Elkaïm, M. T. Sougrati, F. Porcher, F. Damay, J. Rouquette, G. Van Tendeloo, A. Maignan, J. Haines, and C. Martin, Phys. Rev. B **85**, 064102 (2012).

[26]J. de Groot, K. Marty, M. D. Lumsden, A. D. Christianson, S. E. Nagler, S. Adiga, W. J. H. Borghols, K. Schmalzl, Z. Yamani, S. R. Bland, R. de Souza, U. Staub, W. Schweika, Y. Su, and M. Angst, Phys. Rev. Lett. **108**, 037206 (2012).

[27]S. Patankar, S. K. Pandey, V. R. Reddy, A. Gupta, A. Banerjee, and P. Chaddah, Europhys. Lett. **90**, 57007 (2010).

[28]J. Iida, S. Takekawa, and N. Kimizuka, J. Cryst. Growth **102**, 398 (1990).

[29]N. Kimizuka and T. Katsura, J. Solid State Chem. **13**, 176 (1975).

[30]J. Iida, Y. Nakagawa, and N. Kimizuka, J. Phys. Soc. Jpn. **55**, 1434 (1986).

[31]O. Petracic, Z. P. Li, I. V. Roshchin, M. Viret, R. Morales, X. Batlle, and I. K. Schuller, Appl. Phys. Lett. **87**, 222509 (2005).